OPEN ACCESS

Size and Charge Effects on Crossover of Flow Battery Reactants Evaluated by Quinone Permeabilities Through Nafion

To cite this article: Thomas Y. George *et al* 2023 *J. Electrochem. Soc.* **170** 040509

Journal of The Electrochemical Society, 2023 **170** 040509

Size and Charge Effects on Crossover of Flow Battery Reactants Evaluated by Quinone Permeabilities Through Nafion

Thomas Y. George,[1] Emily F. Kerr,[2] Naphtal O. Haya,[3] Abdulrahman M. Alfaraidi,[1] Roy G. Gordon,[1,2] and Michael J. Aziz[1,z]

[1]*Harvard John A. Paulson School of Engineering and Applied Sciences, Cambridge, Massachusetts 02138, United States of America*
[2]*Department of Chemistry and Chemical Biology Harvard University, Cambridge, Massachusetts 02138, United States of America*
[3]*Harvard College, Cambridge, Massachusetts 02138, United States of America*

Organic reactants are promising candidates for long-lifetime redox flow batteries, and synthetic chemistry unlocks a wide design space for new molecules. Minimizing crossover of these molecules through ion exchange membranes is one important design consideration, but the ways in which the crossover rate depends on the structure of the crossing species remain unclear. Here, we contribute a systematic evaluation of size- and charge-based effects on dilute-solution small molecule permeability through the Nafion NR212 cation exchange membrane. We found that increasing the magnitude of charge number z with the same sign as membrane fixed charges, achieved here by successive sulfonation of quinone redox cores, results in more than an order of magnitude permeability reduction per sulfonate. Size-based effects, understood by comparing the Stokes radii of the quinones studied, also reduces permeability with increasing effective molecule size, but doubling the effective size of the redox reactants resulted in a permeability decrease of less than a factor of three.
 [DOI: 10.1149/1945-7111/accb6b]

Manuscript submitted January 6, 2023; revised manuscript received February 28, 2023. Published April 17, 2023. *This paper is part of the JES Focus Issue on Frontiers of Chemical/Molecular Engineering in Electrochemical Energy Technologies in Honor of Robert Savinell.*

Supplementary material for this article is available online

Decarbonization of energy systems is necessary for a sustainable future, and this transformation motivates growth of electrochemical energy storage such as redox flow batteries.[1,2] Water-soluble, redox-active organic molecules (as well as metallorganic species) are increasingly studied for flow battery applications due to their potential for long lifetimes, synthetic tunability, and sustainable feedstocks.[3–5] In a typical flow battery reactor, electrolytes containing these dissolved redox reactants flow through porous electrodes where charge transfer reactions occur. Ions are conducted through an ion exchange membrane, completing the internal electrochemical circuit. The ion exchange membrane is selective against the transport of redox reactants by a combination of charge-based, steric, and energetic effects,[6,7] but unwanted crossover contributes to loss of capacity.[8–10]

The all-vanadium redox flow battery (VRFB) comprises acidic electrolytes with vanadium ions in all four vanadium oxidation states. The ion exchange membrane separates the $V^{3+/2+}$ and $V^{4+/5+}$ electrode reactions. Despite problematic vanadium crossover rates, VRFBs are the most developed flow battery technology, in part because crossover may be recovered by remixing and rebalancing electrolytes.[11] This crossover recovery option is possible because positive and negative electrolytes both use vanadium as the redox reactant. Crossover in redox flow batteries occurs by a combination of diffusion, migration, and (electro)-osmosis transport mechanisms, which have been characterized in the greatest detail for the all-vanadium chemistry.[12–14] Migration and electro-osmosis depend on current density, and all crossover mechanisms depend on the concentration of crossing species absorbed in the membrane pores.[15–18] VRFBs were first developed using proton-conducting cation exchange membranes; more recently anion exchange membranes have been shown to suppress the crossover of vanadium cations by charge-based exclusion.[19,20] This strategy of leveraging the charge exclusion effect of membrane ionic moieties remains an opportunity for new redox flow battery chemistries.

Unlike the VRFB, most organic-based flow batteries (ORFB) use entirely different chemicals as positive and negative electrolytes, and crossover is an irrecoverable loss that, additionally, may result in parasitic side reactions of the crossed-over molecules.[21] Synthetic chemistry enables custom design of organic redox reactants, and this enables crossover mitigation strategies. One such innovation involves tethering redox-active moieties to polymer backbones, using size-exclusion to suppress crossover.[22,23] Oligomerization of redox-active monomers is a related approach to increase redox reactant size.[24–26] A charge-based strategy was employed to decrease viologen crossover in aqueous ORFBs: sulfonate or phosphonate solubilizing groups were attached to the redox active core and paired with a cation exchange membrane, diminishing crossover compared to previous iterations of viologens.[27,28] An extremely low crossover rate was recently reported for an anthraquinone derivative with four sulfonate solubilizing groups in alkaline electrolyte; this may be attributed to a combination of size (branching carbon linkages connecting the redox active core to the solubilizing groups) and charge (four fixed negative charges per molecule).[29]

Crossover rates of some ORFB molecules have been estimated to be very low, but other considerations such as (electro)chemical stability, solubility, mass transport properties, cell voltage, and electrolyte material cost are also critical variables for ORFB development. Consideration of each must be balanced in designing new and promising flow batteries. For example, mass transport properties (e.g. electrolyte viscosity and resulting mass transport coefficients) and solubility may be compromised by a crossover mitigation strategy based on increasing redox reactant size.[21] Here, we contribute a systematic evaluation of size- and charge-based effects on crossover rates in order to inform further design of redox active organic-based electrolytes.

We used quinones soluble in acidic electrolytes as a case study because of the synthetic accessibility of sulfonated and disulfonated hydroquinones and anthraquinones. Hydroquinones were studied instead of benzoquinones due to the chemical instability of benzoquinones in water.[30] Synthesis and use of sulfonated naphthoquinone was attempted, but it was found to be too unstable in water for this

[z]E-mail: maziz@harvard.edu

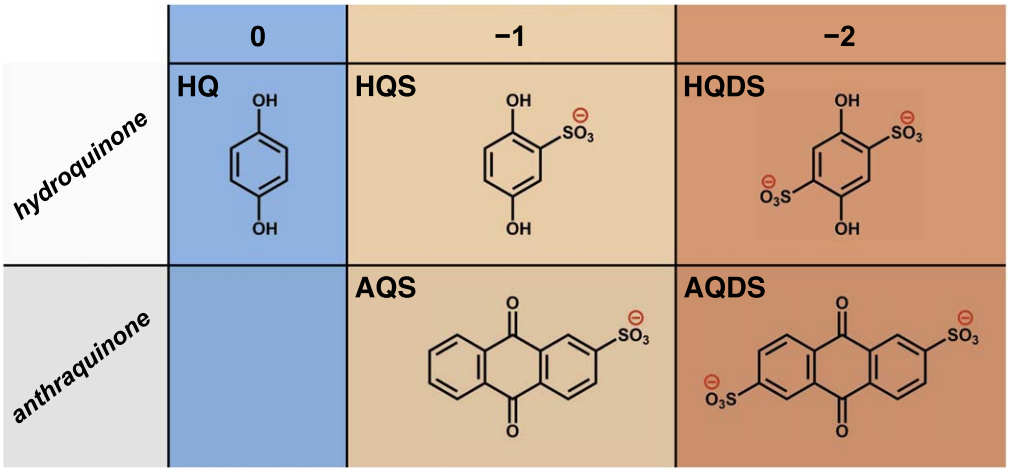

Figure 1. Stick representations of the molecules studied, from top left: 1,4-hydroquinone (HQ), 1,4-hydroquinone-2-sulfonate (HQS), 1,4-hydroquinone 2,5-disulfonate (HQDS), anthraquinone-2-sulfonate (AQS), and anthraquinone-2,6-disulfonate (AQDS).

study (Fig. S1). Figure 1 displays the set of molecules evaluated in this work, categorized by charge number z and by the number of aromatic rings as an indicator of size.

In this work, crossover due to diffusion is evaluated based on permeability through Nafion NR212 cation exchange membranes in dilute conditions (30 mM quinone) and acidic supporting electrolyte (1 M H_2SO_4). Permeability has the same units as diffusivity, but while diffusivity in a membrane depends on the concentration gradient of diffusing species within the membrane itself, permeability depends on the concentration difference of diffusing species between bulk electrolytes on either side of the membrane. Permeability is more readily accessible through experiments and is a useful engineering parameter that describes the crossover rate in a flow battery with a given electrolyte concentration at the zero-current limit.

Nafion is a benchmark cation exchange membrane widely used in redox flow batteries. It possesses a hydrophobic perfluorinated backbone with flexible side chains terminating in hydrophilic sulfonate moieties. The membrane takes up water when immersed in aqueous electrolyte: this water clusters around the ionic groups, and connections between these water domains form pathways for transport.[31] The sulfonate anions of Nafion provide a charge exclusion effect to suppress crossover of co-ions (of the same charge), the sulfonated quinones of this study.

The effective sizes of the quinones were evaluated with rotating disk electrode voltammetry under the same dilute conditions as the permeability experiments. Stokes radii were calculated from measured diffusion coefficients as an estimate of solvated size. We found that the Stokes radii of the hydroquinone species with zero, one, and two sulfonates do not differ by more than 0.1 nm, whereas the permeabilities of these species decrease over a three order of magnitude range with increased negative charge. The permeability of hydroquinone (HQ) through Nafion NR212 is greater than values reported for vanadium,[14] meaning that increasing the magnitude of charge number z is an important strategy for the viability of organic molecules of this size in flow batteries. In contrast, the permeability reduction from hydroquinone-2,5-disulfonic acid (HQDS) to anthraquinone-2,6-disulfonic acid (AQDS), which has over twice the Stokes radius of the former, is less than a factor of 3. Our results show that for a given value of z, drastic changes in size might be needed to have the same effect on permeability as would changing this charge number. The permeability measurements for the set of molecules we present here enables a separate assessment of size- and charge-based effects on crossover rates. By combining these with electrolyte diffusivity measurements, we evaluate the diffusivity/permeability ratio, which has been proposed as a figure of merit for flow batteries, and its dependence on size and charge.

Experimental

Materials.—Nafion NR212 membrane (proton form) was purchased from Ion Power Inc.. Before permeability measurements, membrane pieces were pre-soaked in 1 M H_2SO_4 for at least 12 h at ambient temperature. Concentrated sulfuric acid (KMG Electronic Chemicals, Inc., cleanroom grade) was diluted to 1 M with deionized water (18.2 $M\Omega \cdot cm$) and used as supporting electrolyte in all permeability and electrochemical measurements. Potassium sulfate was purchased from VWR. HQ and HQS (potassium salt) were purchased from Sigma-Aldrich. The sodium salt of AQS was purchased from Sigma-Aldrich and the sodium salt of AQDS was from TCI.

The purchased sodium salts of AQS and AQDS were ion exchanged to potassium before all measurements. First, solutions of the AQS and AQDS sodium salts dissolved in water were passed through a chromatography column packed with Amberlyst 15H resin. In the column, sodium ions in solution exchanged with protons on the resin. Then, 10 M KOH was added dropwise to the resulting solutions until potassium salts of the anthraquinones precipitated from solution. The precipitates were filtered, dried, and used to make solutions for permeability and electrochemical evaluation.

HQDS was synthesized according to procedures in the literature (Fig. S2).[30]

Permeability.—Quinone permeability through Nafion was measured in custom-built glass H-cells (Adams and Chittenden). Each H-cell comprised a "donating" electrolyte solution containing 30 mM quinone potassium salt and 1 M H_2SO_4, a "receiving" electrolyte containing 1 M H_2SO_4 and a concentration of K_2SO_4 to balance the total number of ions on each side of the membrane (Fig. 2a), and Nafion NR212 membrane clamped between the two electrolytes. The volume of each electrolyte solution was 10 ml. H-cells were placed on a multi-channel magnetic sir plate (Scilogex), which kept solutions under agitation for the duration of the experiments. Three replicate H-cells were constructed for each experimental condition.

To measure membrane crossover of quinones from donating to receiving side of the H-cell, aliquots were periodically removed from the receiving side and absorbance spectra of these aliquots were taken using UV–vis spectrophotometry (Agilent). These aliquots were diluted in the cuvette with 1 M H_2SO_4 as needed for the absorbance measurement, and the volume removed from the receiving chamber was replaced with fresh receiving electrolyte (Supplementary Note 1). Concentration of crossed-over quinone in the receiving electrolyte was calculated using a calibration curve for each molecule (Fig. S3).

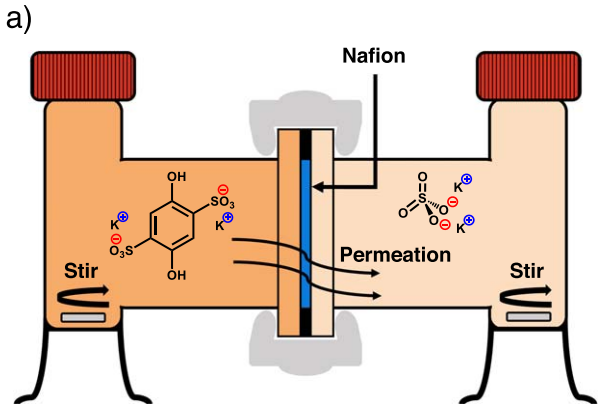

Donating side composition	Receiving side composition
30 mM *x*Q + 1 M H_2SO_4	1 M H_2SO_4
30 mM *x*QS + 1 M H_2SO_4	20 mM K_2SO_4 + 1 M H_2SO_4
30 mM *x*QDS + 1 M H_2SO_4	30 mM K_2SO_4 + 1 M H_2SO_4

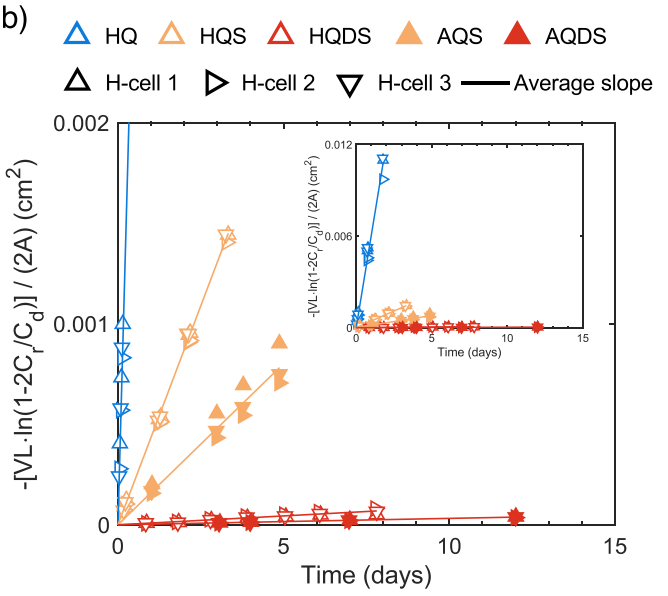

Figure 2. (a) Schematic of H-cell including chemical compositions of donating and receiving electrolytes depending on sulfonation of the quinone, where *x* stands for either H (hydroquinone) or A (anthraquinone). HQDS is depicted as an example. (b) Permeability plot showing three replicate H-cells for each quinone, where the solid lines represent the average permeability from the three replicates.

3-electrode characterization.—Three-electrode measurements were done at ambient temperature with a glassy carbon working electrode (Pine, 5 mm diameter), Ag/AgCl reference electrode (BASi MF-2052) with 3 M NaCl fill solution (0.21 V versus SHE), and platinum wire counter electrode in a glass electrochemical cell (Pine). The working electrode was attached to a rotating shaft for rotating disk electrode experiments (Pine). Electrolytes were degassed with nitrogen before measurements. All solutions studied comprised 30 mM quinone and 1 M H_2SO_4 supporting electrolyte. Cyclic voltammetry and linear sweep voltammetry were performed at 50 mV/s scan rate, and all voltammograms shown are corrected by the subtraction of background current from the same measurement done on a solution of 1 M H_2SO_4.

Results and Discussion

Permeability.—Permeability was evaluated from UV–vis absorbance measurements of crossed-over concentration in the receiving side of H-cells over time. Permeability is defined by Eq. 1, derived from Fick's First Law by assuming equal volumes of solution on each side of the membrane and that diffusion is the only mechanism of transport.

$$P = \frac{\Delta \ln\left[1 - 2\frac{C_r(t)}{C_d(0)}\right]\left(-\frac{VL}{2A}\right)}{\Delta t} \quad [1]$$

In Eq. 1, P is the permeability (cm^2/s), V is the electrolyte volume of each side (10 ml), L is the membrane thickness (50 μm), A is the membrane area (1.979 cm^2), t is time, $C_r(t)$ is the time-dependent concentration of crossed-over species, and $C_d(0)$ is the concentration of crossing species in the donating electrolyte at start of the experiment (30 mM quinone). A finite difference is indicated by Δ. A linear plot in which time is the abscissa and permeability is the slope may be constructed from receiving-side quinone concentration measurements; the linearity is indicative of steady-state diffusion. To avoid a gradient in osmotic pressure, H-cell receiving solutions were designed to balance the total ion concentration on each side of

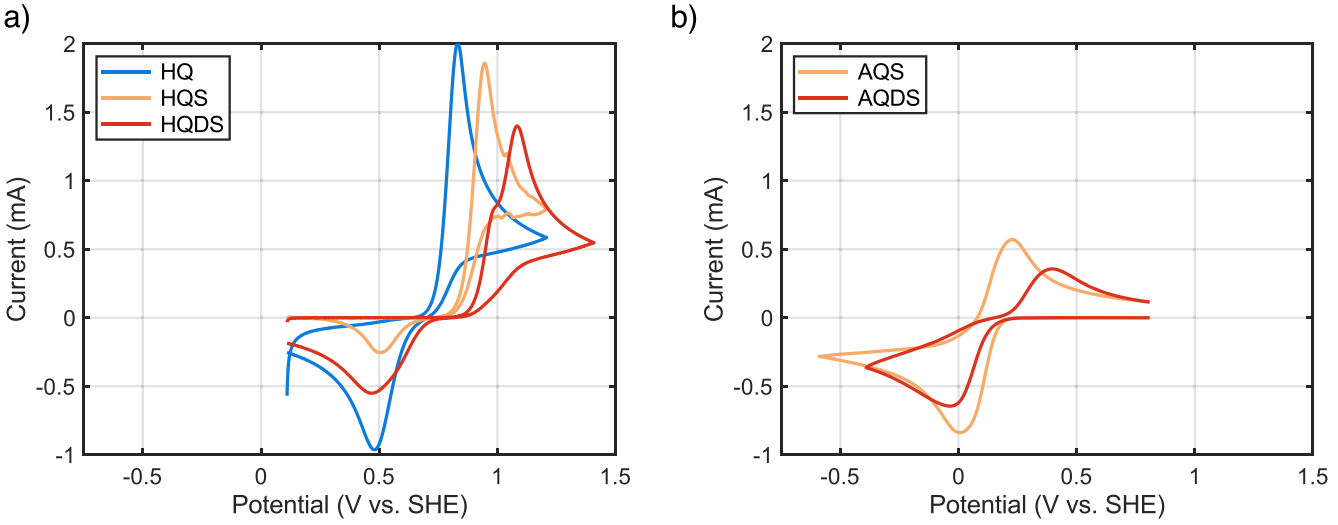

Figure 3. Cyclic voltammograms of 30 mM (a) hydroquinones and (b) anthraquinones in 1 M H_2SO_4 with a scan rate of 50 mV/s. The working electrode is 5 mm diameter glassy carbon.

the membrane (Fig. 2a). After all permeability experiments in this work, the largest change in the amount of electrolyte in a receiving chamber was less than 3% by mass. Figure 2b shows all permeability results from three replicate H-cells for each species studied. The solid lines represent the average permeability from the three replicates. Permeabilities are reported as the average and standard deviation of triplicate experiments for each molecule in Table I.

3-electrode characterization.—Each molecule studied is redox active, as is evident from the oxidation and reduction peaks of their cyclic voltammograms (Fig. 3). Sulfonate is an electron withdrawing group; the redox potentials of the hydroquinones in Fig. 3a and the anthraquinones in Fig. 3b become more positive with sulfonation as expected. Increasing the number of aromatic rings (from hydroquinone to anthraquinone) makes the redox potential less positive. Redox potentials of each molecule, estimated from cyclic voltammetry, are provided in Table SI.

To evaluate the diffusion coefficients of each molecule in 1 M H_2SO_4, we used linear sweep voltammetry at a rotating disk electrode. Linear sweep voltammograms of each species at various disk electrode rotation rates are given in Fig. S4. Each redox reaction reaches a mass transport limited current plateau, the magnitude of which is defined by the Levich equation (Eq. 2).

$$i_l = 0.62nFAD^{2/3}\omega^{1/2}\nu^{-1/6}C \qquad [2]$$

In the Levich equation, n is the number of electrons in the reaction (2 for all reactions here), F is Faraday's constant, A is the geometric area of the working electrode (0.196 cm^2), D is the diffusion coefficient of the redox reactant (cm^2 s^{-1}, to be determined), ω is the rotation rate (s^{-1}, experimentally varied), ν is the kinematic viscosity of 1 M H_2SO_4,[32] and C is the concentration of the redox reactant (30 mM). Thus, the diffusion coefficient of a redox active species is related to the slope of a Levich plot (i_l vs $\omega^1/2$, Fig. 4).

Increasing the charge number z of these molecules through sulfonation without increasing the number of aromatic rings slightly decreases the diffusion coefficient. The effect may be attributed to a combination of stronger intermolecular interaction with the polar solvent (water) and increased molecular weight from the sulfonate groups. Adding aromatic rings to the molecular structure increases size without affecting z; this decreases the diffusion coefficient more appreciably, as visualized in the shallower slopes of the anthraquinone traces compared to those of the hydroquinones in Fig. 4. Diffusion coefficients for each molecule are listed in Table I.

The effect on solvated size of the molecular structure was further investigated by evaluating the Stokes radius of each molecule, using the diffusion coefficients measured in dilute conditions with linear sweep voltammetry. The Stokes radius r_{S_t} is defined by Eq. 3, where k_B is Boltzmann's constant, T is absolute temperature (296 K), and η is the dynamic viscosity of 1 M H_2SO_4.[32]

$$r_{S_t} = \frac{k_B T}{6\pi\eta D} \qquad [3]$$

This equation defines the radius of a hard sphere (i.e. a simple model of a molecule and its solvation shell) diffusing through a medium without interacting with the solvent or other diffusing particles. Its assumptions are reasonable for dilute solutions such as those evaluated in this study. Stokes radii are listed for each molecule alongside diffusion coefficients in Table I.

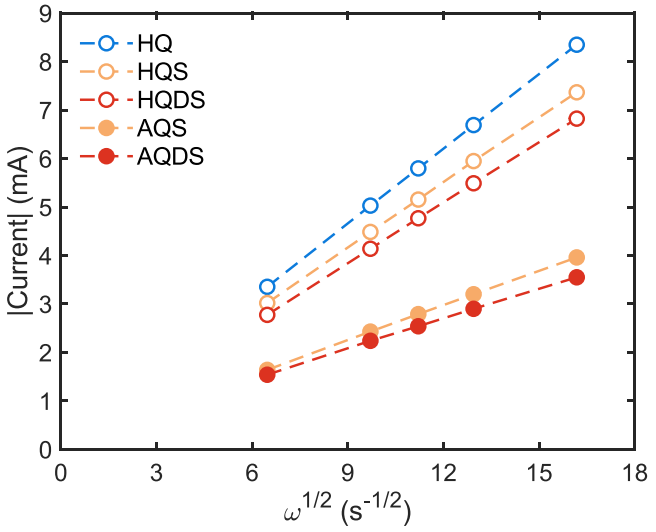

Figure 4. Levich plot for each redox reactant. Absolute values of currents are shown to plot hydroquinone oxidation and anthraquinone reduction in the same quadrant.

Discussion.—The data collected in this study support the existing heuristics that increasing size and increasing the magnitude of charge number z (with the same sign as membrane fixed charge) diminish membrane permeability and thereby suppress crossover. Further, the systematic variation of size and charge enable assessment of the two effects separately. Each successive sulfonation of hydroquinone diminishes its permeability by greater than one order of magnitude while increasing its Stokes radius by less than 0.1 nm, as shown in Fig. 5a. These data emphasize the benefit of increasing the magnitude of redox reactant z with the same sign as membrane fixed charges.

The influence of charge exclusion is further elucidated by Fig. 5b, which displays diffusivity/permeability ratios for each molecule, a crossover-related figure of merit proposed in the flow battery community.[25,26] Diffusivity of HQ in the 1 M H_2SO_4 electrolyte is less than 100 times its permeability through the tortuous membrane pores. Crossover of HQ is unconstrained by charge exclusion effects, and may even by accelerated by favorable hydrophobic interactions with the Nafion polymer. Its diffusivity in electrolyte is therefore relatively close to its permeability across the membrane phase, compared to the D/P ratios of the anions studied. The D/P ratios of the anions increase with z because permeability is sensitive to charge exclusion whereas diffusivity, by comparison, is not.

Donnan exclusion is a simple model to explain this charge selectivity. At equilibrium, the electrochemical potential of a given ionic species is equal between the membrane phase (solution within the membrane pores) and the contacting electrolyte. For ideal

Table I. Summary of molecule properties and permeabilities.

Molecule	z	Stokes radius (nm)	Diffusivity in 1 M H_2SO_4 (cm^2/s)	Permeability (cm^2/s)
HQ	0	0.31	6.4×10^{-6}	$7.0 \times 10^{-8} \pm 4.2 \times 10^{-9}$
HQS	−1	0.35	5.6×10^{-6}	$5.0 \times 10^{-9} \pm 8.3 \times 10^{-11}$
HQDS	−2	0.40	4.9×10^{-6}	$1.0 \times 10^{-10} \pm 1.7 \times 10^{-11}$
AQS	−1	0.88	2.2×10^{-6}	$1.9 \times 10^{-9} \pm 2.0 \times 10^{-10}$
AQDS	−2	0.91	2.2×10^{-6}	$3.7 \times 10^{-11} \pm 3.4 \times 10^{-12}$

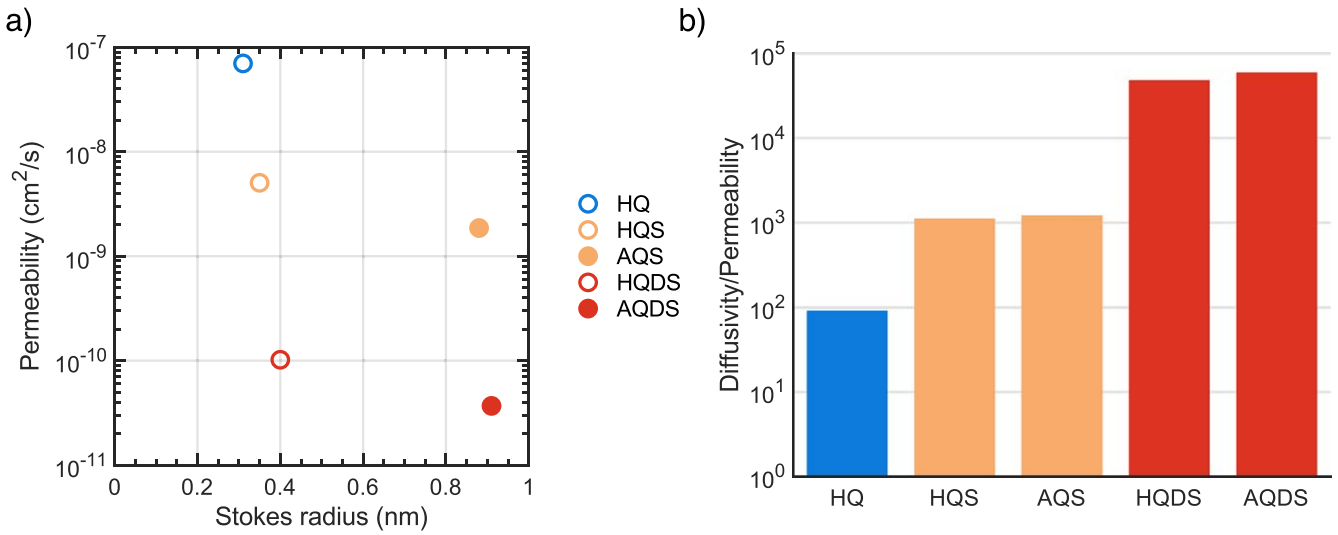

Figure 5. (a) Permeability vs Stokes radius for quinones of different charge numbers. (b) Diffusivity/permeability ratio, a dimensionless crossover figure of merit, for each molecule.

solutions of ions, the concentration of a co-ion in the membrane phase (*e.g.* a sulfonated quinone in Nafion) may be approximated by considering the concentration of membrane fixed charges and the condition of electroneutrality, without involving any other membrane properties (Supplementary Note 2).[9,33] To fulfill this condition, the co-ion concentration in the membrane phase must be lower than in the contacting electrolyte: this is the Donnan exclusion effect. The effect is strengthened when the valence of co-ions is higher, such that fewer dianions (*e.g.* HQDS) may enter the pores of Nafion than single anions like HQS, for a given concentration of the anionic species in the contacting electrolyte. HQ is not an ion and thus is not subject to Donnan exclusion, so by the Donnan model it may have the same concentration in the membrane phase as in the electrolyte phase (30 mM).

Permeability is directly proportional to concentration of crossing species in the membrane phase at a given electrolyte concentration. At 30 mM concentration in the contacting electrolyte, HQDS and AQDS may have a factor-of-ten lower concentration in Nafion than HQS and AQS by Donnan exclusion (Fig. S5). As a dilute-solution first approximation, Donnan exclusion is a useful model. The measurements show an even larger reduction in permeability between the mono- to disulfonated species, meaning that additional selectivity mechanisms must be involved.

Charge exclusion effects are weakened as electrolyte concentration increases and approaches the concentration of membrane fixed charges. For a membrane such as Nafion, Donnan exclusion can have a significant effect on membrane phase co-ion concentration even at 1 M of co-ions, but the effect would be slight for a hypothetical 10 M electrolyte (Fig. S5).[9] The effects of size exclusion, a different strategy, may be enhanced as the size of the crossing species approaches the membrane pore size. Pursuing a size exclusion strategy for small molecules (with a current state-of-the art ion exchange membrane) will have drawbacks related to mass transport, and may incur added penalties of higher cost and lower solubility. The charge exclusion strategy may afford added benefits, such as improving water solubility and suppressing intermolecular collisions that cause deleterious side reactions.

For the development of new redox flow battery electrolytes, electrochemical and transport parameters (including permeability) are routinely assessed at dilute concentration, but concentrated solution effects on these parameters may become relevant in a practical battery where high energy density is desired. To understand crossover when concentrated electrolytes are involved, concentration-dependent changes in membrane water content, ion association equilibria, and interactions between all species in solution should be considered.[6,13] Concentrated solution effects are expected to further complicate the influence of molecular structure on crossover.

This study takes the perspective of molecule design, using Nafion as a benchmark membrane. However, significant progress may also be made by approaching the problem from the membrane perspective. Uncharged size exclusion separators may offer lower cost and resistance compared with ion exchange membranes,[34] but in this case designing molecules for size exclusion is crucial. Moving in the opposite direction, increasing membrane ion exchange capacity may enhance charge exclusion, although high ion exchange capacity membranes tend to face issues related to swelling,[35] which can have a harmful impact on crossover, so designing optimal ion exchange membrane structures remains a productive research direction. In addition, polymers of intrinsic microporosity are recently emerging for flow batteries, and these membranes may offer enhanced size exclusion compared to traditional ion exchange membranes, and may also be functionalized with ionic groups for charge exclusion.[36–39] There is an opportunity for the synergistic development of membranes and molecules to benefit the progress of sustainable electrochemical technology.

Conclusions

Crossover has been a persistent issue in the development of electrochemical reactors such as redox flow batteries, but the growing field of organic-based redox reactants has unlocked mitigation strategies leveraging charge and size exclusion. We have presented a systematic study to consider these effects separately in order to inform design of new redox active chemistries and their selection for electrochemical devices.

Quinones are presented as a case study: the number of aromatic rings (hydroquinone vs anthraquinone) tunes size whereas installation of sulfonate moieties nearly independently tunes charge number z. Diffusivity and Stokes radius (effective size) of these molecules were assessed with voltammetry and combined with permeability measurements through Nafion NR212 cation exchange membranes to evaluate size and charge effects. As shown in Fig. 5, for the hydroquinones and anthraquinones studied, the doubling of Stokes radius from about 0.4 nm to about 0.8 nm that comes from changing from a one-ring molecule to a three-ring molecule with the same charge state cuts the permeability by less than a factor of 3, whereas adding each negatively charged sulfonate increases the Stokes radius by <0.1 nm but cuts the permeability by more than an order of magnitude. For these small molecules in dilute solution, although we observe both size and charge effects on permeability, the effect of

size on crossover is marginal compared to the effect of charge-based exclusion with ion exchange membranes.

Acknowledgments

The information, data, or work presented herein was funded in part by U.S. DOE award DE-AC05-76RL01830 through PNNL subcontract 535264. This material is based upon work supported by the National Science Foundation Graduate Research Fellowship Program under Grant No. DGE 1745303 (supporting T.Y.G.). Any opinions, findings, and conclusions or recommendations expressed in this material are those of the authors and do not necessarily reflect the views of the National Science Foundation. The authors thank Dr. Diana D. Porcellinis, Eric M. Fell, Anton M. Graf, and Dr. Kiana Amini for helpful discussions.

ORCID

Thomas Y. George https://orcid.org/0000-0002-0159-8521
Roy G. Gordon https://orcid.org/0000-0001-5980-268X
Michael J. Aziz https://orcid.org/0000-0001-9657-9456

References

1. L. Trahey et al., "Energy storage emerging: A perspective from the Joint Center for Energy Storage Research." *Proc. Natl. Acad. Sci. U.S.A.*, **117**, 12550 (2020).
2. J. Rugolo and M. J. Aziz, "Electricity storage for intermittent renewable sources." *Energy Environ. Sci.*, **5**, 7151 (2012).
3. X. Wei et al., "Materials and systems for organic redox flow batteries: status and challenges." *ACS Energy Lett.*, **2**, 2187 (2017).
4. A. Saal, T. Hagemann, and U. S. Schubert, "Polymers for battery applicationsactive materials, membranes, and binders." *Advanced Energy Materials*, **11**, 2001984 (2020).
5. D. G. Kwabi, Y. Ji, and M. J. Aziz, "Electrolyte lifetime in aqueous organic redox flow batteries: a critical review." *Chem. Rev.*, **120**, 6467 (2020).
6. A. R. Crothers, R. M. Darling, A. Kusoglu, C. J. Radke, and A. Z. Weber, "Theory of multicomponent phenomena in cation-exchange membranes: part I. thermodynamic model and validation." *J. Electrochem. Soc.*, **167**, 013547 (2020).
7. V. Freger, "Selectivity and polarization in water channel membranes: Lessons learned from polymeric membranes and CNTs." *Faraday Discussions*, **209**, 371 (2018).
8. A. R. Crothers, R. M. Darling, D. I. Kushner, M. L. Perry, and A. Z. Weber, "Theory of multicomponent phenomena in cation-exchange membranes: part III. transport in vanadium redox-flow-battery separators." *J. Electrochem. Soc.*, **167**, 013549 (2020).
9. R. Darling, K. Gallagher, W. Xie, L. Su, and F. Brushett, "Transport property requirements for flow battery separators." *J. Electrochem. Soc.*, **163**, A5029 (2016).
10. K. W. Knehr, E. Agar, C. R. Dennison, A. R. Kalidindi, and E. C. Kumbur, "A transient vanadium flow battery model incorporating vanadium crossover and water transport through the membrane." *J. Electrochem. Soc.*, **159**, A1446 (2012).
11. L. Wei, X. Z. Fan, H. R. Jiang, K. Liu, M. C. Wu, and T. S. Zhao, "Enhanced cycle life of vanadium redox flow battery via a capacity and energy efficiency recovery method." *Journal of Power Sources*, **478**, 228725 (2020).
12. D. I. Kushner, A. R. Crothers, A. Kusoglu, and A. Z. Weber, "Transport phenomena in flow battery ion-conducting membranes." *Current Opinion in Electrochemistry*, **21**, 132 (2020).
13. A. R. Crothers, R. M. Darling, A. Kusoglu, C. J. Radke, and A. Z. Weber, "Theory of multicomponent phenomena in cation-exchange membranes: part II. transport model and validation." *J. Electrochem. Soc.*, **167**, 013548 (2020).
14. R. M. Darling, A. Z. Weber, M. C. Tucker, and M. L. Perry, "The influence of electric field on crossover in redox-flow batteries." *J. Electrochem. Soc.*, **163**, A5014 (2016).
15. R. A. Elgammal, Z. Tang, C. N. Sun, J. Lawton, and T. A. Zawodzinski, "Species uptake and mass transport in membranes for vanadium redox flow batteries." *Electrochimica Acta*, **237**, 1 (2017).
16. Z. Tang, R. Svoboda, J. S. Lawton, D. S. Aaron, A. B. Papandrew, and T. A. Zawodzinski, "Composition and conductivity of membranes equilibrated with solutions of sulfuric acid and vanadyl sulfate." *J. Electrochem. Soc.*, **160**, F1040 (2013).
17. H. S. Cho, M. Ohashi, and J. W. V. Zee, "Absorption behavior of vanadium in Nafion®." *Journal of Power Sources*, **267**, 547 (2014).
18. J. S. Lawton, A. Jones, and T. Zawodzinski, "Concentration dependence of VO 2+ crossover of nafion for vanadium redox flow batteries." *J. Electrochem. Soc.*, **160**, A697 (2013).
19. R. M. Darling, J. D. Saraidaridis, C. Shovlin, M. Fortin, L. A. Murdock, and B. C. Benicewicz, "The influence of current density on transport of vanadium cations through membranes with different charges." *J. Electrochem. Soc.*, **168**, 040516 (2021).
20. R. M. Darling, J. D. Saraidaridis, C. Shovlin, and M. Fortin, "Vanadium transport through cation and anion exchange membranes." *ECS Trans.*, **97**, 215 (2020).
21. M. L. Perry, J. D. Saraidaridis, and R. M. Darling, "Crossover mitigation strategies for redox-flow batteries." *Current Opinion in Electrochemistry*, **21**, 311 (2020).
22. T. Hagemann, J. Winsberg, M. Grube, I. Nischang, T. Janoschka, N. Martin, M. D. Hager, and U. S. Schubert, "An aqueous all-organic redox-flow battery employing a (2,2,6,6-tetramethylpiperidin-1-yl)oxyl-containing polymer as catholyte and dimethyl viologen dichloride as anolyte." *Journal of Power Sources*, **378**, 546 (2018).
23. T. Janoschka, N. Martin, U. Martin, C. Friebe, S. Morgenstern, H. Hiller, M. D. Hager, and U. S. Schubert, "An aqueous, polymer-based redox-flow battery using non-corrosive, safe, and low-cost materials." *Nature*, **527**, 78 (2015).
24. M. J. Baran, M. N. Braten, E. C. Montoto, Z. T. Gossage, L. Ma, E. Chénard, J. S. Moore, J. Rodríguez-López, and B. A. Helms, "Designing redox-active oligomers for crossover-free, nonaqueous redox-flow batteries with high volumetric energy density." *Chem. Mater.*, **30**, 3861 (2018).
25. K. H. Hendriks, S. G. Robinson, M. N. Braten, C. S. Sevov, B. A. Helms, M. S. Sigman, S. D. Minteer, and M. S. Sanford, "High-performance oligomeric catholytes for effective macromolecular separation in nonaqueous redox flow batteries." *ACS Central Science*, **4**, 189 (2018).
26. S. E. Doris, A. L. Ward, A. Baskin, P. D. Frischmann, N. Gavvalapalli, E. Chénard, C. S. Sevov, D. Prendergast, J. S. Moore, and B. A. Helms, "Macromolecular design strategies for preventing active-material crossover in non-aqueous all-organic redox-flow batteries." *Angew. Chem.*, **129**, 1617 (2017).
27. S. Jin, E. M. Fell, L. Vina-Lopez, Y. Jing, P. W. Michalak, R. G. Gordon, and M. J. Aziz, "Near neutral pH redox flow battery with low permeability and long-lifetime phosphonated viologen active species." *Adv. Energy Mater.*, **10**, 2000100 (2020).
28. C. Debruler, B. Hu, J. Moss, J. Luo, and T. L. Liu, "A sulfonate-functionalized viologen enabling neutral cation exchange, aqueous organic redox flow batteries toward renewable energy storage." *ACS Energy Lett.*, **3**, 663 (2018).
29. M. Wu, M. Bahari, Y. Jing, K. Amini, E. M. Fell, T. Y. George, R. G. Gordon, and M. J. Aziz, "Highly stable, low redox potential quinone for aqueous flow batteries." *Batteries & Supercaps*, **5**, e202200009 (2022).
30. J. B. Gerken, C. W. Anson, Y. Preger, P. G. Symons, J. D. Genders, Y. Qiu, W. Li, T. W. Root, and S. S. Stahl, "Comparison of quinone-based catholytes for aqueous redox flow batteries and demonstration of long-term stability with tetrasubstituted quinones." *Adv. Energy Mater.*, **10**, 2000340 (2020).
31. A. Kusoglu and A. Z. Weber, "New insights into perfluorinated sulfonic-acid ionomers." *Chem. Rev.*, **117**, 987 (2017).
32. F. H. Rhodes and C. B. Barbour, "The viscosities of mixtures of sulfuric acid and water." *Industrial and Engineering Chemistry*, **15**, 850 (1923).
33. J. M. M. Peeters, "Characterization of nanofiltration membranes." *Ph.D. Thesis*, University of Twente (1997).
34. Z. Liang, N. H. Attanayake, K. V. Greco, B. J. Neyhouse, J. L. Barton, A. P. Kaur, W. L. Eubanks, F. R. Brushett, J. Landon, and S. A. Odom, "A comparison of separators vs membranes in nonaqueous redox flow battery electrolytes containing small molecule active materials." *ACS Appl. Energy Mater.*, **4**, 5443 (2021).
35. C. R. Peltier, Z. Rhodes, A. J. Macbeth, A. Milam, E. Carroll, G. W. Coates, and S. D. Minteer, "Suppressing crossover in nonaqueous redox flow batteries with polyethylene-based anion-exchange membranes." *ACS Energy Lett.*, **7**, 4118 (2022).
36. C. Ye et al., "Long-life aqueous organic redox flow batteries enabled by amidoxime-functionalized ion-selective polymer membranes." *Angewandte Chemie - International Edition*, **61**, e202207580 (2022).
37. C. Ye et al., "Development of efficient aqueous organic redox flow batteries using ion-sieving sulfonated polymer membranes." *Nat. Commun.*, **13**, 3184 (2022).
38. R. Tan et al., "Hydrophilic microporous membranes for selective ion separation and flow-battery energy storage." *Nat. Mater.*, **19**, 195 (2020).
39. P. Zuo et al., "Sulfonated microporous polymer membranes with fast and selective ion transport for electrochemical energy conversion and storage." *Angewandte Chemie - International Edition*, **59**, 9564 (2020).